Effect of Misfit at Implant-Level Framework and Supporting Bone on Internal Connection Implants: Mechanical and Finite Element Analysis

Marco Toia, DDS[1]/Michele Stocchero, DDS, PhD[1]/Yohei Jinno, DDS, PhD[1]/
Ann Wennerberg, DDS, PhD[2]/Jonas P. Becktor, DDS, PhD[1]/Ryo Jimbo, DDS, PhD[3]/
Anders Halldin, MS, PhD[4]

Purpose: To evaluate the effect of misfit at implant-level fixed partial dentures (ILFPDs) and marginal bone support on the generation of implant cracks. **Materials and Methods:** This in vitro study included a mechanical fatigue test and finite element analysis. A mechanical cycling loading test was performed using 16 experimental models, each consisting of two parallel implants subdivided into four groups based on the misfit and the supporting bone condition. The framework, firmly seated at implants, was dynamically loaded vertically with a force of 1,600/160 N and 15 Hz for 1×10^6 cycles. Optical microscope, scanning electron microscope (SEM), and computed tomography three-dimensional (CT-3D) analyses were performed to detect impairments. Finite element models, representing the setups in the mechanical fatigue test, were used to represent the fatigue life. **Results:** None of the mechanical components presented distortion or fracture at the macroscopic level during the test. In a microscopy evaluation, the fatigue test revealed scratches visible in the inner part of the conical portion of the implants regardless of the groups. SEM and CT-3D analysis revealed one implant from the misfit/no bone loss group with a microfracture in the inner part of the conical interface. The simulated effective stress levels in the coronal body were higher in the misfit groups compared with the no misfit groups. The misfit groups presented effective stress levels, above 375 MPa, that penetrated the entire wall thickness. The no bone loss group presented an effective stress level above 375 MPa along its axial direction. In the no misfit group, the area presenting effective stress levels above 375 MPa in the conical connection was larger for the bone loss group compared with the no bone loss group. **Conclusion:** This study confirmed that implant fracture is an unlikely adverse event. A clear pattern of effective distribution greater than fatigue limit stresses could be noticed when the misfit was present. The dynamic load simulation demonstrated that the crack is more likely to occur when implants are fully supported by marginal bone compared with a bone loss scenario. Within the limitations of this study, it is speculated that marginal bone loss might follow the appearance of an undetected crack. Further research is needed to develop safe clinical protocols with regard to ILFPD. Int J Oral Maxillofac Implants 2019;34:320–328. doi: 10.11607/jomi.6965

Keywords: CAD/CAM, finite element analysis, implant fracture, implant level, misfit

The use of implant-supported fixed prosthetic rehabilitation for partial edentulism is supported

[1]Department of Oral and Maxillofacial Surgery and Oral Medicine, Malmö University, Sweden.
[2]Department of Prosthodontics, Sahlgrenska Academy, University of Gothenburg, Sweden.
[3]Department of Applied Prosthodontics, Graduate School of Biomedical Sciences, Nagasaki University, Nagasaki, Japan.
[4]I3tex, Gothenburg, Sweden.

Correspondence to: Dr Marco Toia, Department of Oral and Maxillofacial Surgery and Oral Medicine, Faculty of Odontology, Malmö University, Carl Gustavs väg 34, SE 205 06, Malmö, Sweden. Email: marco.toia@mau.se

©2019 by Quintessence Publishing Co Inc.

by robust evidence on long-term success rates with a small amount of marginal bone resorption.[1–3] Although high survival rates of fixed partial dentures (FPDs) have been reported, the incidence of biologic and technical complications is nevertheless relevant to discuss. In a meta-analysis by Pjetursson et al,[4] the patient-centered esteemed 5-year FPD complication rate was 38.7%.

To prevent technical complications in screw-retained constructions, a passive fit between the components is advocated.[5] A perfect fit was defined as simultaneous contact of all the fitting surfaces with the absence of strain before load application.[6,7] However, this represents an ideal condition, and it is hardly reproducible in the clinical reality. The generation of misfits between the components is inevitable throughout the prosthetic procedures, starting from the impression to the construction delivery.[8]

Different techniques have been suggested to minimize the inaccuracy in the production of the framework such as splinted impressions,[9,10] low fusing metal casts,[11] and computer-aided design/computer-aided manufacturing (CAD/CAM) technology.[12–14]

Nevertheless, when the fit is inadequate, uneven stresses and strains are introduced in the interface between the framework and implant. This condition has been indicated to be one of the causing factors for mechanical complications, such as screw/abutment loosening or fractures, framework fracture, and, in the worst scenarios, implant fracture and implant loss.[15]

It is unclear whether an implant fracture is a consequence or a cause of marginal bone loss.[16,17] Metal cracks in the implant may be caused by unfavorable bending stresses when excessive resorption of the supporting bone has occurred.[18] On the other hand, a preexisting undetected crack might be the cause of marginal bone loss.[19,20] In fact, the stress distribution on the implant body when misfit is applied to implants with different supporting bone levels is unknown.

Thus, the present study aimed to evaluate the effects of misfit at implant-level fixed partial dentures (ILFPDs) and supporting bone level on the generation of implant cracks with a coupled method of a mechanical test and finite element analysis (FEA).

MATERIALS AND METHODS

Mechanical Fatigue Test

A mechanical cycling loading test was performed using an experimental model consisting of two parallel implants with a diameter of 3.5 mm and a length of 11 mm (Astra Tech Implant System Osseospeed TX, Dentsply Sirona Implants). The implants were embedded in epoxy resin cylinder with a diameter of 10 mm and a length of 13 mm and firmly seated in an aluminum block (60 × 60 × 40 mm).

Two metal blocks were manufactured to mimic the perfect fit and the misfit condition, defined as the discrepancy between the implant longitudinal axis and the restorative longitudinal axis,[21] as follows:

- *No misfit:* The distance between the center of the two implants was 35.0 mm.
- *Misfit:* The distance between the center of the two implants was 35.2 mm.

Moreover, to detect the effect of supporting bone level, implants were placed with different embedding depths:

- *No bone loss:* The implant shoulder was placed at 0.0 ± 0.5 mm above the surface of the epoxy resin (nominal level).
- *Bone loss:* The implant shoulder was placed at 3.0 ± 0.5 mm above the nominal level according to ISO std. 14801:2007, simulating the worst bone loss scenario (Fig 1).

Sixteen computer-numeric-controlled (CNC)-milled Titanium Bridge Type rigid frameworks (42 × 10 × 7.5 mm) (Atlantis Superstructures, Dentsply Sirona) were fabricated from the same file with a distance between the center of the two implants of 35 mm. The accuracy of the frameworks is granted by CNC-milling manufacturing, which was demonstrated to have small variability and high precision with an amount of error of less than 10 μm.[22,23]

The total length of the conical connection was 2 mm, and the depth of the framework into the implant was 1.2 mm. The frameworks, free from antirotational interlocking, were screwed with a torque of 20 Ncm into the implants. Radiographs were taken after the final position of the framework to check the presence of misfit.

Experimental models (n = 16) were subdivided into four groups based on the misfit condition and the supporting bone condition, as shown in Fig 1.

The framework was externally dynamically loaded vertically in the center using a loading machine (Electropuls E3000, Instron) with a force of 160 to 1,600 N at 15 Hz for 1×10^6 cycles. The rigidity of the framework minimizes unfavorable bar deformation, inducing an equal vertical load and negligible bending moment to the implant-abutment interface. Therefore, the expected dynamic load on each implant varied between 80 and 800 N. After loading, the embedded implants were removed from the metal block and examined through an optical microscope with a ×50 magnification lens (ZEISS Stemi 2000-C Stereo Microscope).

Afterward, the samples were investigated using a scanning electron microscope (SEM) (Hitachi TM3000, Hitachi). Implants were placed in a tilted fashion into the vacuum camera. Each implant was rotated 60 degrees and analyzed three times to obtain a complete view of the conical inner side.

As a final examination, the samples were analyzed with an industrial computed tomography three-dimensional (CT-3D) X-Ray Measuring System (ZEISS Metrotom 800 CT system). The measurement conditions were set at 95 kV and 80 μA. The primary x-ray beam was filtered by a 0.5-mm-thick aluminum target. Eight hundred fifty high-resolution (scan resolution of 10.17 μm, voxel dimension) radiographs were collected, by spinning the sample in autofocus mode, in no more than 60 minutes. Special software (Volume
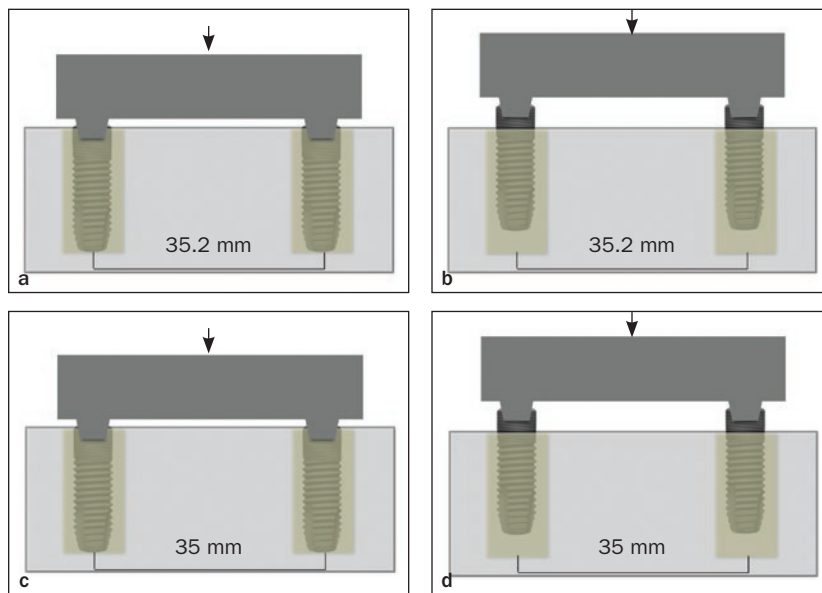
Fig 1 Experimental models subdivided into four groups based on implant vertical position and misfit: (a) misfit/no bone loss, (b) misfit/bone loss, (c) no misfit/no bone loss, and (d) no misfit/bone loss. Arrow represents the direction of the loading.
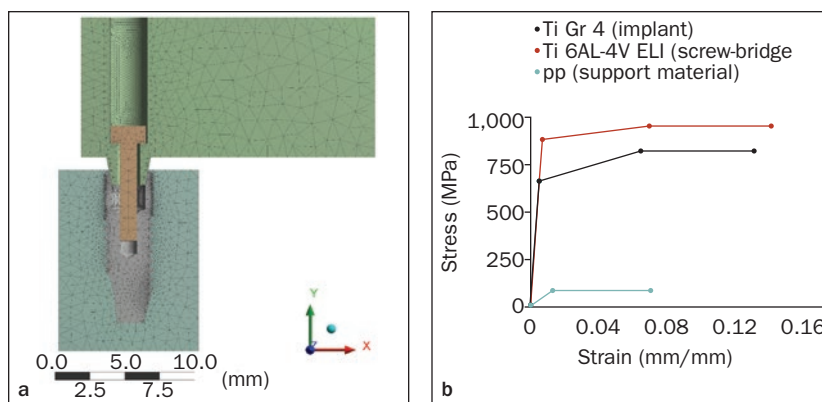

Fig 2 (a) FEA model simulated for one implant side. (b) Multilinear material properties.

Graphics) was used to reconstruct the two-dimensional (2D) images into a 3D volume.

Finite Element Analysis

To investigate the stress distribution at the implant, finite element models, representing the setups in mechanical fatigue tests, were developed in ANSYS 18.2 (ANSYS).

Taking advantage of the symmetry of the model, only one implant side was simulated (Fig 2a). To capture the mechanical properties of the metallic components, the simulations were performed using multilinear material properties (Fig 2b). This model captures the increase in stress between yield and ultimate strength. In addition, this material model limits the simulated stress to the ultimate stress.[24] The interface between the framework and the implant was modeled with a friction coefficient of 0.3.[25] To reduce the simulation time, the interface between the framework and the abutment screw was modeled as a frictionless connection, while the interface between the implant and support material was modeled as a bonded one.

The meshes were generated using the ANSYS default settings with a denser mesh size of 0.075 mm in the implant-framework interface. These settings resulted in 0.13×10^6 nodes and 0.08×10^6 elements of the bone loss condition and 0.19×10^6 nodes and 0.12×10^6 elements of the no bone loss condition.

To analyze how the mesh density affected the results, the model that comprised a misfit of 0.2 mm and 0 mm bone loss was modeled with an increased mesh of 0.05 mm and with a reduced mesh of 0.1 mm at the implant-framework interface.

Tightening of the framework was simplified in the FEA model to only include a screw preload of 250 N and neglecting any shear forces arising due to screw torqueing.[26] This simplification does not suppose to affect the results in the coronal part of the implant. To replicate the experimental setup, the preload was applied first; thereafter, a maximum load of 800 N was applied on the implant at the implant-framework interface.

The stress levels were analyzed by the mean von Mises stress criterion. The alternating stress range (σ_r) was defined as the difference in von Mises stress

Fig 3 Stress-life diagram (S-N) of titanium Gr 4 with a UTS of 820 MPa, reflecting the mechanical proprieties of the implant used in the in vitro fatigue test. The S-N curve of TI Gr 4 with UTS of 820 MPa (red line) was derived from an offset of the S-N curve of Ti Gr 4 with a UTS of 470 MPa (green).[28]
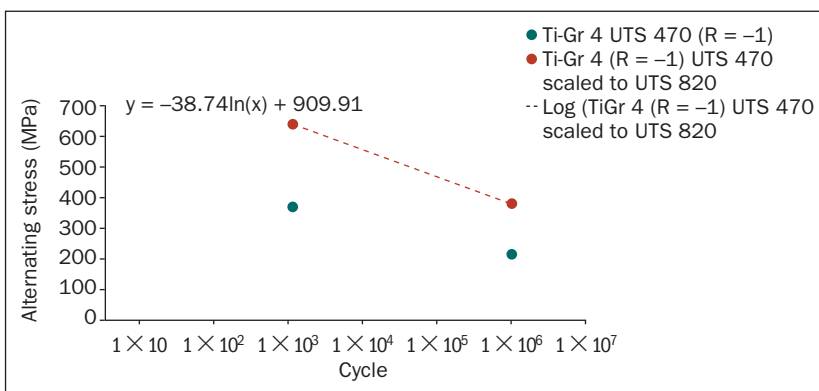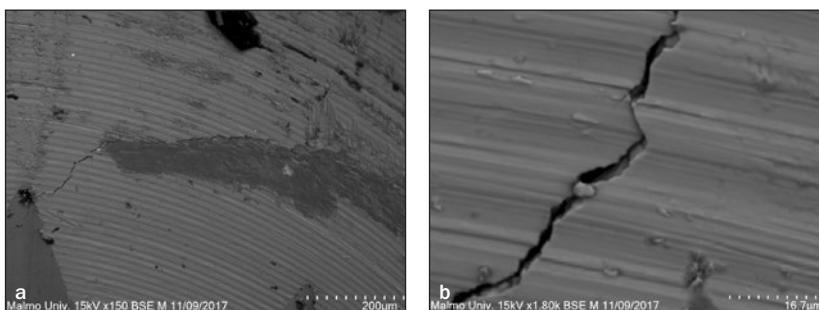

Fig 4 SEM analysis revealed one implant from the misfit/no bone loss group with a microfracture in the inner part of the conical interface ([a] × 150 and [b] × 1.80K magnification).

between 800 N (maximum stress level σ_{max}) and 80 N (minimum stress level σ_{min}):

$$\sigma_r = \sigma_{max} - \sigma_{min}.$$

The alternating stress amplitude (σ_a) is defined as:
$$\sigma_a = \sigma_r / 2.$$

The mean stress level (σ_m) is defined as:

$$\sigma_m = (\sigma_{max} + \sigma_{min})/2.$$

In this simulation, the modified Goodman theory was used to assess fatigue life.[24]

The mean stress correction by Goodman results in an effective fully reversed stress amplitude (σ_{er}) that can be used to compare with an existing stress life diagram (S-N) of fully reversed load ($R = -1$) of titanium Gr 4:

$$\sigma_{er} = \sigma_a \times \left(1 - \frac{\sigma_m}{\sigma_u}\right)$$

where σ_u is the ultimate tensile strength (UTS) of the material.[27]

The effective fully reversed stress amplitude σ_{er} found in this simulation was compared with a stress-life diagram (S-N) of titanium Gr 4 with a UTS of 820 MPa, reflecting the mechanical properties of the implant used in the in vitro fatigue test. The S-N curve of Ti Gr 4 with UTS of 820 MPa used in this study was

derived from an offset of the S-N curve of Ti Gr 4 with a UTS of 470 MPa presented by Chandran (Fig 3).[28] The offset was calculated as the ratio between UTS 820 and UTS 470.

RESULTS

Mechanical Fatigue Test

Prior to torqueing the framework to the implant, a misfit was clearly visible in both misfit groups and also detectable on radiographic images after the final torque fixation.

None of the mechanical components presented distortion or fracture at the macroscopic level during the test. After the test, no microfractures of the prosthetic screws were detected.

The microscopy evaluation demonstrated some scratches visible in the inner part of the conical portion of the implants regardless of the groups. SEM and CT-3D analysis revealed one implant out of eight from the misfit/no bone loss group with a microfracture in the inner part of the conical interface (Figs 4 and 5). Scratches, wear, minor damages, and titanium debris were a common finding at the interface of the majority of the implants regardless of the groups in SEM analysis.

Finite Element Analysis

Decreasing the mesh did not dramatically affect the von Mises stress level at the circumferential opening at the coronal portion of the implant as presented in Fig 6. Therefore, to reduce simulation time, a mesh size
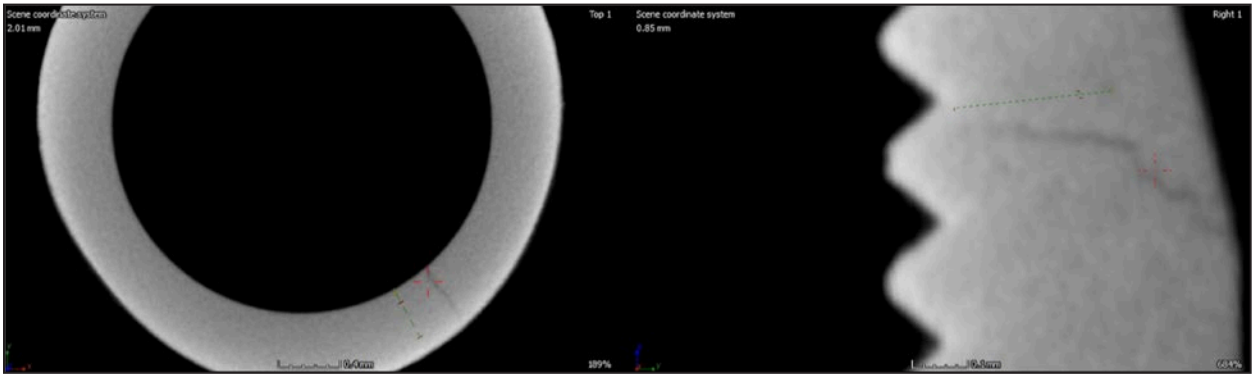
Fig 5 *(Above)* Computed tomography 3D (CT-3D) x-ray analysis revealed one implant from the misfit/no bone loss group with a microfracture in the inner part of the conical interface.
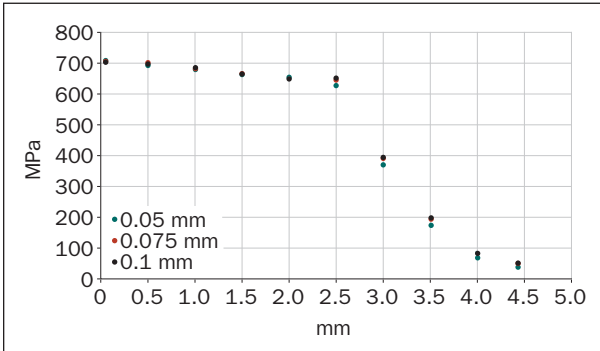
Fig 6 *(Left)* Von Mises stress level at the circumferential opening, starting from the misfit contact side, at the coronal portion of the implant of three different mesh sizes (green 0.05 mm, red 0.075 mm, black 0.1 mm).
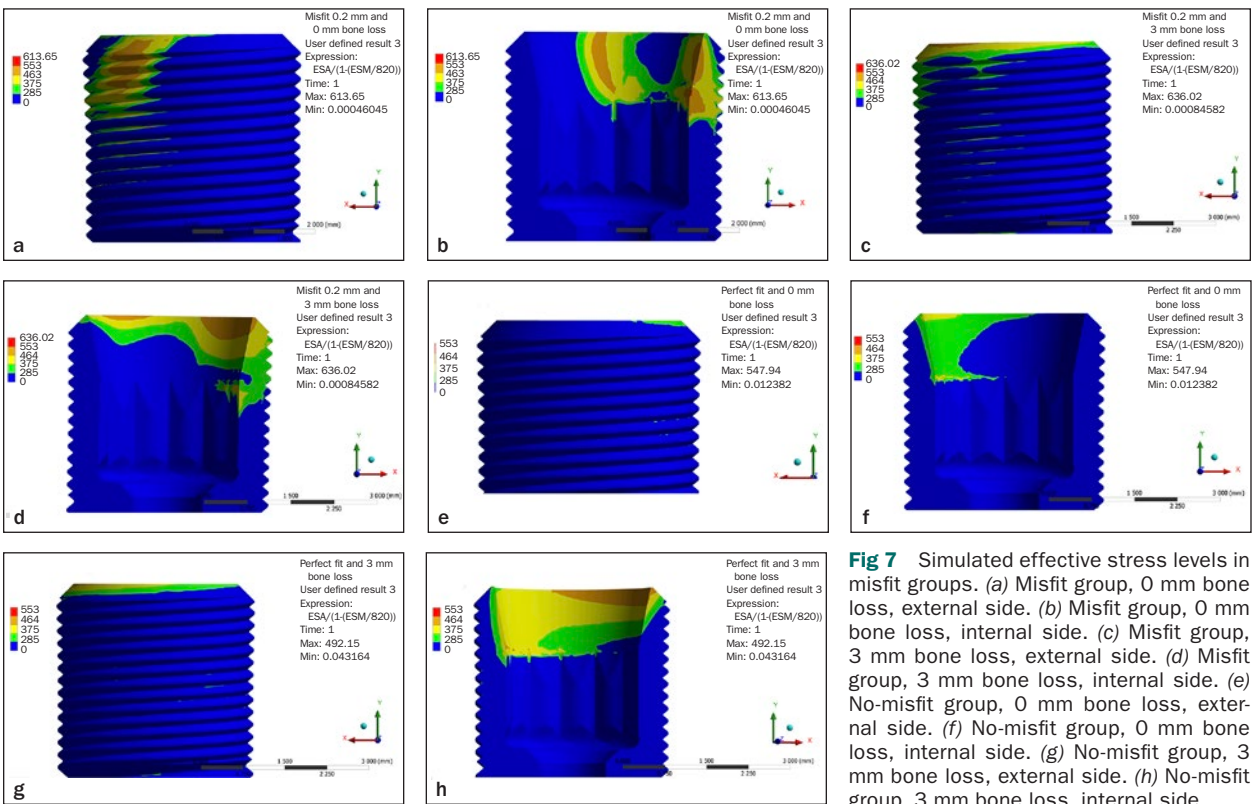

Fig 7 Simulated effective stress levels in misfit groups. *(a)* Misfit group, 0 mm bone loss, external side. *(b)* Misfit group, 0 mm bone loss, internal side. *(c)* Misfit group, 3 mm bone loss, external side. *(d)* Misfit group, 3 mm bone loss, internal side. *(e)* No-misfit group, 0 mm bone loss, external side. *(f)* No-misfit group, 0 mm bone loss, internal side. *(g)* No-misfit group, 3 mm bone loss, external side. *(h)* No-misfit group, 3 mm bone loss, internal side.

of 0.075 mm in the implant-framework interface was used for all other simulations.

The simulated effective stress levels in the coronal body were higher in the misfit groups compared with the no misfit groups.

Effective stress lower than 375 MPa represents a lifetime ($N > 1 \times 10^6$ cycles) (Fig 3). The misfit groups presented effective stress levels, above 375 MPa, that penetrated the entire wall thickness. The no bone loss group presented an effective stress level above

375 MPa along its axial direction (Figs 7a to 7h). In the no misfit group, the area presenting effective stress levels above 375 MPa in the conical connection was larger for the bone loss group compared with the no bone loss group (Fig 7).

DISCUSSION

In this study, the effect of misfit at screw-retained CNC-milled frameworks when connected at the implant level was investigated with a coupled method of an in vitro fatigue model and FEA.

It has been reported that conical implant-abutment connections for screw-retained restorations exhibit better continuity in yield forces,[29–31] and possess high rigidity[32] with low risk for leakage compared with external or internal butt joints.[33,34]

Arguably, internal conical connection may present mechanical disadvantages because of the reduced coronal wall thickness, having a decreased bearing capacity.[18,35]

To rehabilitate partial edentulism with screw-retained FPDs, the placement of a multiunit abutment between the implant and the framework has previously been recommended.[36] Such an abutment would protect the implant from overload by compensating the misfit between the components.[37]

Implant-level restorations have been developed by Lewis at al[38] to treat patients with limited intraoral vertical space. Few studies investigated the clinical outcome of implant-level reconstructions,[39] especially in conical connection implants.[40,41] Some authors suggested that ILFPDs are one of the most challenging situations; yet, they are frequently used in daily practice to reduce cost and improve esthetics.[42,43] This type of reconstruction requires highly accurate prosthetic procedures in order to not induce critical stresses in the implant-framework interface.[44] Unfavorable stress levels and metal fatigue increase the risk of mechanical complications.[20,45]

In the present study, a cycling load model was developed so that repeated stresses predisposed the implants to fail under fatigue. This model was considered to be a more clinically relevant approach than static fracture tests.[46] The magnitude of load was chosen in accordance with the maximum occlusal force recorded in humans with an implant-supported reconstruction in the posterior area of the jaw.[47,48]

A 200-µm misfit between the implants and the framework was introduced. In a recent review, such an amount of discrepancy was considered as a very poor fit and not clinically acceptable.[7] However, some authors reported that a misfit of more than 200 µm has minor influence on clinical outcomes.[49,50]

It has been reported that a kind of bone adaptation occurs when a framework is connected to an implant, and peri-implant bone stress will increase with a certain degree of remodeling. In vitro, in vivo, and clinical studies demonstrate that implant displacement occurs, reducing the total amount of misfit and total compensation of approximately 20 µm.[13] Still, this potential displacement is more pronounced if the connection between the framework and implant is fixed in the early phase of healing. Further, no study evaluated if the effect of misfit on an implant-level setup in a conical connection implant has a mechanical or biologic impact.[13]

The results from the fatigue loading model revealed that only one implant out of 32 presented signs of material failure. One crack (Fig 4) was detected in the SEM analysis at the inner surface of one implant out of eight in the misfit/no bone loss group. This finding was also confirmed in the CT-3D analysis, where the crack engaged the implant wall (Fig 5).

Repetitive applied force generating stress levels below yield might result in material failure as a result of the load cycles. Goodman's mean correction theory was used to evaluate the fatigue life of the implant. This theory calculates an effective stress, based on the stress amplitude and mean stress, that could be compared to experimental S-N curves of fully reversed load; ie, the mean stress is 0.

Generally, there are different theories used to analyze the influence of a fluctuating stress. Goodman's theory has a conservative approach and underestimates the fatigue life, and the choice was made to incorporate a potential error in the model setup.[24] This might explain why there was only one sample of the physical test that resulted in a crack while the FEA presented a lifetime less than 1×10^6 cycles above 375 MPa. The objective was to identify if there is an increased risk of fatigue in the implant with increased misfit with two different supports during cyclic load. Therefore, all four groups were simulated using the same FEA setup. Hence, this simulation neglects fatigue life dependencies such as surface treatment and stress concentration factors (ie, notch effects). However, these factors are assumed to provide similar dependences of all four models.

The FEA performed in this study revealed a clear pattern of effective stress concentration along all implant-framework connections. This finding is in accordance with a previous study,[21] in which the effect of misfit at the connection between the implant and two-unit ILFPD was simulated.

The fatigue limit, at 1×10^6 cycles, of Ti Gr 4 has been reported to be approximately 50% of UTS.[51] This is in the same range used in this study (Fig 3), indicating that the offset approach of the fatigue data presented

by Chandran seems reasonable.[28] Visually, the simulated effective stress is presented in Fig 7, where the green color represents the fatigue limit of titanium at 1×10^6 cycles. In the misfit/no bone loss group, a vertical region of effective stresses above the fatigue limit was presented. The high location of these high stresses seems to penetrate through the wall thickness that might initiate a fatigue crack (Fig 7a). These high simulated effective stresses of the misfit/no bone loss group coincide with the location of the crack detected at the SEM and at the CT-3D (Figs 4 and 5).

The bone loss groups presented areas of high simulated effective stresses that seemed not to penetrate through the wall thickness to the same extent as found in the misfit/no bone loss group.

From the present FEA findings, preserved supporting bone level (no bone loss) seemed to increase the risk of vertical fracture compared with the bone loss groups, when there is a misfit. One explanation might be that, in the absence of full support (bone loss), the implant more easily adjusts to the final position, hence reducing the simulated effective stress. This might explain why no cracks were found in the samples of the bone loss groups after the fatigue test. In addition, the discrepancy between results from the mechanical test and FEA is not totally surprising since it was previously observed that fatigue tests may fail to identify the crack initiation site.[52] Furthermore, the screw preload maintained a minimum force of 250 N in the conical portion of the implant that decreased the alternating stress. This could explain why only one sample presented a crack despite the high load of 800 N.

Arguably, another factor that could have influenced the in vitro results was the possibility to maintain the discrepancy during the cycling loading. It could be speculated that the resin embedded blocks inserted in the metal block could have compensated the misfit when the load was applied.

Moreover, the number of cycles applied in the fatigue model, which corresponded to 1.5 years of functional load,[46] might not have been sufficient to trigger a fatigue failure.[28]

A limited incidence of implant fracture has been reported in different systematic reviews to occur in less than 1% of all implants during a 5-year period.[18,53,54] Nonetheless, this evidence is likely to be underestimated,[19] and it is reported to appear more frequently in a multiunit partial restoration than in a full-arch replacement.[15]

It must be said that, among the limitations of this experimental setup, the implants were placed in a parallel position. Different results can be expected in terms of fractures when an angulation between the implants is present. Furthermore, the misfit condition was generated only as a horizontal interimplant discrepancy, but in the clinical reality, it may occur in all three dimensions. Such a condition of angular misfit may be relevant, since it was observed that it provokes more bone stress in comparison to only horizontal and vertical ones.[55] Moreover, aggravating factors may include the type of occlusion and the patient's parafunctional habits, which may persist in long-term time intervals and repetitive stress concentrations, above the yield limit, and could provoke minor, moderate, or major mechanical failures such as implant fracture.[15]

This in vitro experiment seems to confirm the clinical evidence that implant fracture is an uncommon adverse event, even when a large framework misfit is present. However, the location of high-stress areas highlighted in the computational model must be seriously considered by the clinician when a multiunit ILFPD is chosen as the treatment plan.

Clinicians must follow a precise prosthetic protocol to reduce the potential degree of misfit, such as splinting impression, and use methods to validate the master model.[9–12] Moreover, if unfavorable clinical conditions such as parafunctional habits and/or an interimplant angulation that exceeds the conical total axis deviation persist, an abutment-level connection should be recommended instead of implant-level ones.[33]

The present findings suggest that implant fractures are more likely to occur when implants are fully supported by marginal bone, hence supporting the claim that cracks appear before bone loss. Therefore, it might be speculated that a secondary bacterial contamination of undetected fractured surfaces would cause a rapid bone breakdown.

Future clinical studies should evaluate the incidence of implant fracture comparing implant-level restorations with different setups, including abutment-level restoration.

CONCLUSIONS

With the limitation of this setup, this study confirmed that implant fracture is an unlikely/adverse event. A clear pattern of effective stress distribution greater than fatigue limit stresses could be noticed when the misfit was present. The dynamic load simulation demonstrated that the crack is more likely to occur when implants are fully supported by marginal bone, compared with a bone loss scenario. Within the limitations of this study, it is speculated that marginal bone loss might follow the appearance of an undetected crack. Further research is needed to develop safe clinical protocols with regard to ILFPD.

ACKNOWLEDGMENTS

REFERENCES

1. Wennström JL, Ekestubbe A, Gröndahl K, Karlsson S, Lindhe J. Oral rehabilitation with implant-supported fixed partial dentures in periodontitis-susceptible subjects. A 5-year prospective study. J Clin Periodontol 2004;31:713–724.
2. Wennerberg A, Jemt T. Complications in partially edentulous implant patients: A 5-year retrospective follow-up study of 133 patients supplied with unilateral maxillary prostheses. Clin Implant Dent Relat Res 1999;1:49–56.
3. Brägger U, Karoussis I, Persson R, Pjetursson B, Salvi G, Lang N. Technical and biological complications/failures with single crowns and fixed partial dentures on implants: A 10-year prospective cohort study. Clin Oral Implants Res 2005;16:326–334.
4. Pjetursson BE, Brägger U, Lang NP, Zwahlen M. Comparison of survival and complication rates of tooth-supported fixed dental prostheses (FDPs) and implant-supported FDPs and single crowns (SCs). Clin Oral Implants Res 2007;18(suppl 3):97–113.
5. Quirynen M, van Steenberghe D. Bacterial colonization of the internal part of two-stage implants. An in vivo study. Clin Oral Implants Res 1993;4:158–161.
6. Abduo J, Lyons K, Bennani V, Waddell N, Swain M. Fit of screw-retained fixed implant frameworks fabricated by different methods: A systematic review. Int J Prosthodont 2011;24:207–220.
7. Katsoulis J, Takeichi T, Sol Gaviria A, Peter L, Katsoulis K. Misfit of implant prostheses and its impact on clinical outcomes. Definition, assessment and a systematic review of the literature. Eur J Oral Implantol 2017;10(suppl 1):121–138.
8. Wee AG, Aquilino SA, Schneider RL. Strategies to achieve fit in implant prosthodontics: A review of the literature. Int J Prosthodont 1999;12:167–178.
9. Vigolo P, Fonzi F, Majzoub Z, Cordioli G. An evaluation of impression techniques for multiple internal connection implant prostheses. J Prosthet Dent 2004;92:470–476.
10. Lee H, So JS, Hochstedler JL, Ercoli C. The accuracy of implant impressions: A systematic review. J Prosthet Dent 2008;100:285–291.
11. Manzella C, Bignardi C, Burello V, Carossa S, Schierano G. Method to improve passive fit of frameworks on implant-supported prostheses: An in vitro study. J Prosthet Dent 2016;116:52–58.
12. Kapos T, Evans C. CAD/CAM technology for implant abutments, crowns, and superstructures. Int J Oral Maxillofac Implants 2014;29(suppl):117–136.
13. Abduo J, Judge RB. Implications of implant framework misfit: A systematic review of biomechanical sequelae. Int J Oral Maxillofac Implants 2014;29:608–621.
14. Miyazaki T, Hotta Y, Kunii J, Kuriyama S, Tamaki Y. A review of dental CAD/CAM: Current status and future perspectives from 20 years of experience. Dent Mater J 2009;28:44–56.
15. Eckert SE, Meraw SJ, Cal E, Ow RK. Analysis of incidence and associated factors with fractured implants: A retrospective study. Int J Oral Maxillofac Implants 2000;15:662–667.
16. Shemtov-Yona K, Rittel D. Identification of failure mechanisms in retrieved fractured dental implants. Eng Fail Anal 2014;38:58–65.
17. Virdee P, Bishop K. A review of the aetiology and management of fractured dental implants and a case report. Br Dent J 2007;203:461–466.
18. Chrcanovic BR, Kisch J, Albrektsson T, Wennerberg A. Factors influencing the fracture of dental implants. Clin Implant Dent Relat Res 2018;20:58–67.
19. Narra N, Antalainen AK, Zipprich H, Sándor GK, Wolff J. Micro-computed tomography-based assessment of retrieved dental implants. Int J Oral Maxillofac Implants 2015;30:308–314.
20. Takeshita K, Toia M, Jinno Y, et al. Implant vertical fractures provoked by laboratory procedures: A finite element analysis inspired from clinical cases. Implant Dent 2016;25:361–366.
21. Jimbo R, Halldin A, Janda M, Wennerberg A, Vandeweghe S. Vertical fracture and marginal bone loss of internal-connection implants: A finite element analysis. Int J Oral Maxillofac Implants 2013;28:e171–e176.
22. de França DG, Morais MH, das Neves FD, Carreiro AF, Barbosa GA. Precision fit of screw-retained implant-supported fixed dental prostheses fabricated by CAD/CAM, copy-milling, and conventional methods. Int J Oral Maxillofac Implants 2017;32:507–513.
23. Svanborg P, Skjerven H, Carlsson P, Eliasson A, Karlsson S, Ortorp A. Marginal and internal fit of cobalt-chromium fixed dental prostheses generated from digital and conventional impressions. Int J Dent 2014;2014:534382.
24. Bader Q, Kadum E. Mean stress correction effects on the fatigue life behavior of steel alloys by using stress life approach theories. Int J Eng Technol 2014;10:50.
25. Jörn D, Kohorst P, Besdo S, Rücker M, Stiesch M, Borchers L. Influence of lubricant on screw preload and stresses in a finite element model for a dental implant. J Prosthet Dent 2014;112:340–348.
26. Halldin A, Dahlström M. Optimization of preload and torsion by using a unique abutment screw design for each implant platform size. Clin Oral Implants Res 2013;24:162–163.
27. Niesłony A, Böhm M. Mean stress effect correction using constant stress ratio S–N curves. Int J Fatigue 2013;52:49–56.
28. Chandran KR. A physical model and constitutive equations for complete characterization of S-N fatigue behavior of metals. Acta Materialia 2016;121:85–103.
29. Suzuki H, Hata Y, Watanabe F. Implant fracture under dynamic fatigue loading: Influence of embedded angle and depth of implant. Odontology 2016;104:357–362.
30. Vigolo P, Gracis S, Carbonini F, Mutinelli S; AIOP (Italian Academy of Prosthetic Dentistry) Clinical Research Group. Internal- vs external-connection single implants: A retrospective study in an Italian population treated by certified prosthodontists. Int J Oral Maxillofac Implants 2016;31:1385–1396.
31. Norton MR. An in vitro evaluation of the strength of an internal conical interface compared to a butt joint interface in implant design. Clin Oral Implants Res 1997;8:290–298.
32. Sumi T, Braian M, Shimada A, et al. Characteristics of implant-CAD/CAM abutment connections of two different internal connection systems. J Oral Rehabil 2012;39:391–398.
33. Berberi A, Tehini G, Rifai K, Bou Nasser Eddine F, Badran B, Akl H. Leakage evaluation of original and compatible implant-abutment connections: In vitro study using Rhodamine B. J Dent Biomech 2014;5:1758736014547143.
34. Schmitt CM, Nogueira-Filho G, Tenenbaum HC, et al. Performance of conical abutment (Morse Taper) connection implants: A systematic review. J Biomed Mater Res A 2014;102:552–574.
35. Lee JH, Huh YH, Park CJ, Cho LR. Effect of the coronal wall thickness of dental implants on the screw joint stability in the internal implant-abutment connection. Int J Oral Maxillofac Implants 2016;31:1058–1065.
36. Adell R, Lekholm U, Brånemark PI, et al. Marginal tissue reactions at osseointegrated titanium fixtures. Swed Dent J Suppl 1985;28:175–181.
37. Helldén L, Ericson G, Elliot A, et al. A prospective 5-year multicenter study of the Cresco implantology concept. Int J Prosthodont 2003;16:554–562.
38. Lewis SG, Llamas D, Avera S. The UCLA abutment: A four-year review. J Prosthet Dent 1992;67:509–515.
39. Göthberg C, Gröndahl K, Omar O, Thomsen P, Slotte C. Bone and soft tissue outcomes, risk factors, and complications of implant-supported prostheses: 5-Years RCT with different abutment types and loading protocols. Clin Implant Dent Relat Res 2018;20:313–321.

40. Hjalmarsson L, Smedberg JI, Pettersson M, Jemt T. Implant-level prostheses in the edentulous maxilla: A comparison with conventional abutment-level prostheses after 5 years of use. Int J Prosthodont 2011;24:158–167.

41. Barbier L, Abeloos J, De Clercq C, Jacobs R. Peri-implant bone changes following tooth extraction, immediate placement and loading of implants in the edentulous maxilla. Clin Oral Investig 2012;16:1061–1070.

42. Eliasson A, Wennerberg A, Johansson A, Ortorp A, Jemt T. The precision of fit of milled titanium implant frameworks (I-Bridge) in the edentulous jaw. Clin Implant Dent Relat Res 2010;12:81–90.

43. Hjalmarsson L, Smedberg JI. A 3-year retrospective study of Cresco frameworks: Preload and complications. Clin Implant Dent Relat Res 2005;7:189–199.

44. Choi JH, Lim YJ, Yim SH, Kim CW. Evaluation of the accuracy of implant-level impression techniques for internal-connection implant prostheses in parallel and divergent models. Int J Oral Maxillofac Implants 2007;22:761–768.

45. Tagger-Green N, Horwitz J, Machtei EE, Peled M. [Implant fracture: A complication of treatment with dental implants—review of the literature]. Refuat Hapeh Vehashinayim (1993) 2002;19:19–24, 68. [Article in Hebrew]

46. Coray R, Zeltner M, Özcan M. Fracture strength of implant abutments after fatigue testing: A systematic review and a meta-analysis. J Mech Behav Biomed Mater 2016;62:333–346.

47. Sathyanarayana HP, Premkumar S, Manjula WS. Assessment of maximum voluntary bite force in adults with normal occlusion and different types of malocclusions. J Contemp Dent Pract 2012;13:534–538.

48. Nishigawa K, Bando E, Nakano M. Quantitative study of bite force during sleep associated bruxism. J Oral Rehabil 2001;28:485–491.

49. Jemt T, Book K. Prosthesis misfit and marginal bone loss in edentulous implant patients. Int J Oral Maxillofac Implants 1996;11:620–625.

50. Jokstad A, Shokati B. New 3D technologies applied to assess the long-term clinical effects of misfit of the full jaw fixed prosthesis on dental implants. Clin Oral Implants Res 2015;26:1129–1134.

51. Boyer HE (ed). Atlas of Fatigue Curves. Materials Park, Ohio: ASTM International, 1986.

52. Yamaguchi S, Yamanishi Y, Machado LS, et al. In vitro fatigue tests and in silico finite element analysis of dental implants with different fixture/abutment joint types using computer-aided design models. J Prosthodont Res 2018;62:24–30.

53. Berglundh T, Persson L, Klinge B. A systematic review of the incidence of biological and technical complications in implant dentistry reported in prospective longitudinal studies of at least 5 years. J Clin Periodontol 2002;29(suppl 3):197–212; discussion 232–233.

54. Brägger U, Aeschlimann S, Bürgin W, Hämmerle CH, Lang NP. Biological and technical complications and failures with fixed partial dentures (FPD) on implants and teeth after four to five years of function. Clin Oral Implants Res 2001;12:26–34.

55. Winter W, Mohrle S, Holst S, Karl M. Bone loading caused by different types of misfits of implant-supported fixed dental prostheses: A three-dimensional finite element analysis based on experimental results. Int J Oral Maxillofac Implants 2010;25:947–952.